

Mateusz NIEDŹWIEDŹ*, Marek BARA*, Władysław SKONECZNY*

THE INFLUENCE OF SURFACE FREE ENERGY ON TRIBOLOGICAL PROPERTIES OF OXIDE LAYERS FORMED ON ALUMINIUM ALLOY EN AW-5251

WPLYW SWOBODNEJ ENERGII POWIERZCHNIOWEJ NA WŁAŚCIWOŚCI TRIBOLOGICZNE WARSTW TLENKOWYCH WYTWARZANYCH NA STOPIE ALUMINIUM EN AW-5251

Key words:

anodising, surface free energy, wetting angle, T-17 tester, composite materials.

Abstract

This paper presents the influence of the parameters of the formation of oxide layers on the surface free energy and the tribological properties of these layers. The layers were formed electrochemically on aluminium alloy EN AW-5251, with variable values of electrolyte temperature and current density. A three-component electrolyte was used to produce oxide layers. The surface free energy was determined by the droplet deposition method by measuring the wetting angles, while the van Oss-Chaunhury-Good method was used for the calculations. Tribological tests were performed on a T-17 tribological tester under conditions of technically dry friction for reciprocating motion. T7W composite was used as a specimen in tribological tests.

Słowa kluczowe:

anodowanie, wolna energia powierzchniowa, kąt zwilżania, tester T-17, materiały kompozytowe.

Streszczenie:

W artykule przedstawiono wpływ parametrów wytwarzania warstw tlenkowych na swobodną energię powierzchniową oraz właściwości tribologiczne tych warstw. Warstwy zostały wytworzone na stopie aluminium EN AW-5251 metodą elektrochemiczną, przy zmiennych wartościach temperatury elektrolitu oraz gęstości prądowej. Do wytwarzania warstw tlenkowych zastosowano elektrolit trójskładnikowy. Swobodna energia powierzchniowa wyznaczona została metodą osadzonej kropli poprzez pomiar kątów zwilżania, natomiast do obliczeń zastosowano metodę van Ossa-Chaunhury'ego-Gooda. Testy tribologiczne przeprowadzono na testerze tribologicznym T-17 w warunkach tarcia technicznie suchego dla ruchu posuwisto-zwrotnego. W testach tribologicznych jako próbki użyto kompozytu T7W.

INTRODUCTION

Oxide layers formed on aluminium alloys using the hard anodising method are widely used in the structures of industrial machines. Hard anodising on aluminium alloys is most frequently used to increase the mechanical strength of elements of machine parts, while maintaining the advantages of aluminium alloys, which undoubtedly include low weight of the material and good electrical conductivity [L. 1, 2]. The mechanical properties of oxide layers can be modified by changing the parameters of the anodising process, such as current density, electrolyte temperature, and process time [L. 3]. The condition of the upper layer of the material is very important for the durability and reliability of elements of interacting

machine parts. This is caused by the action of processes and phenomena that appear as a result of friction [L. 4]. The mechanical and tribological properties of the material are strongly influenced by the energy state of the upper layer. The material wetting angle, and thus the surface free energy, significantly contributes to the improvement of the lubrication of the materials, reducing friction [5 = 7]. Tribology increasingly draws attention to the energetic properties of upper layer formation, which can significantly influence the occurrence of processes and phenomena such as abrasive wear and the ability to create a sliding film [L. 8, 9].

The above paper presents the influence of the surface free energy of Al_2O_3 layers on the tribological properties of these layers. The tests were carried out

* University of Silesia in Katowice, Faculty of Computer Science and Materials Science, Institute of Technology and Mechatronics, Department of Surface Layers Technology, ul. Śnieżna 2, 41-200 Sosnowiec, Poland, e-mail: mateusz.niedzwiedz@us.edu.pl.

using the droplet deposition method. The mechanical properties of oxide layers formed were also investigated (SGS, microhardness, and surface morphology).

RESEARCH METHODOLOGY

Research material

The specimens for the test of the sliding couple were made of T7W. T7W is a PTFE-based composite with a dispersion phase in the form of powdered technical carbon. The exact chemical composition of the composite is unknown due to the manufacturer's patent protection. This material is characterised by a very low value of the friction coefficient when it interacts with metals. It is widely used in hydraulic and pneumatic friction systems, especially in the production of guide rings used in pneumatic actuators.

In the tests, plates made of EN AW-5251 aluminium alloy with an area of 0.1 dm² were used as counter-specimens. **Table 1** shows the chemical composition of alloy EN AW-5251.

The counter-specimens were etched in KOH and then in HNO₃. Water solutions of the following acids were used as the electrolyte: H₂SO₄, C₂H₂O₄, and C₈H₆O₄. The parameters of the anodising process are shown in **Table 2**. Anodising was carried out at a constant electrical charge density of 180 [A · min/dm²].

After the completed anodising process, the counter-specimens were rinsed in distilled water for 1 hour.

Table 1. Chemical composition of alloy EN AW-5251

Tabela 1. Skład chemiczny stopu EN AW-5251

Elemental symbol	Mg	Mn	Si	Fe	Cu	Zn	Cr	Ti	Al
Chemical composition in [%]	1.90	0.26	0.20	0.32	0.05	0.01	0.02	0.02	97.2

Table 2. Parameters of the anodising process

Tabela 2. Parametry procesu anodowania

Determination of the counter-specimen	Current density I [A/dm ²]	Temperature T [K]	Process time t [min]
A	3	293	60
B	3	298	60
C	3	303	60
D	2	298	90
E	4	298	45

Test stand

The tribological tests were carried out with the use of a pin-plate friction node mounted on a T-17 tribological tester (**Fig. 1**). The tester is used to test the friction force and wear of couples that perform reciprocating motion. The tribological tests were carried out in dry friction conditions, at a constant ambient temperature (25±1°C)

and relative air humidity (60±10%). A constant sliding speed of 0.2 m/s and constant unit pressures of 1 MPa were applied. The tests were carried out on a friction distance of 15 km. The linear wear of the node and friction force during the tribological test were recorded with a Catman 4.5 program.

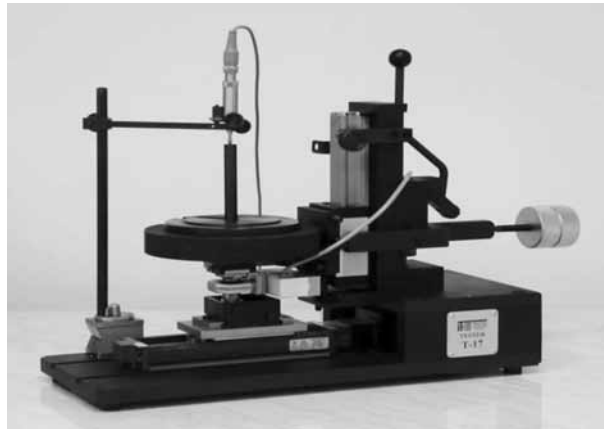


Fig. 1. T-17 tribological tester (the Institute for Sustainable Technologies, Tribology Department, Radom)

Rys. 1. Tester tribologiczny T-17 (Instytut Technologii Eksploatacji, Zakład Tribologii, Radom)

The hardness of the oxide layer, which depends on the production parameters, was measured. The measurements were made on metallographic specimens. The cavities were made with a Hanemann microhardness tester with a Vickers indenter using a load of 0.3 N.

Three cavities, seven repetitions each, were made in each specimen. The images of surface morphology of Al₂O₃ oxide layers were made with a scanning microscope (SEM). A magnification of 5000x was used to analyse the surface. The images of the microstructure of T7W were made on an Olympus motorised system microscope at a magnification of 200x.

SFE was measured based on the determined wetting angle for three reference liquids. Polar (glycerine, water) and non-polar (diiodomethane) liquids were used. The measurement was made by applying 10 drops of liquid on the surface of the counter-specimen with a micropipette. Each of the drops had a volume of 0.5 μl . Images of each drop were made with a camera. The wetting angle for each drop was measured using See System Standard 6.3 software. The two angles with the largest deviations were discarded, and the program calculated an arithmetic mean based on the remaining ones. The average wetting angle was then used to calculate SFE using the van Oss-Chaunhury-Good method. Two polar (water, glycerine) and one non-polar (diiodomethane) liquids are used in this method.

The surface geometric structure (SGS) was studied in order to determine the roughness. SGS measurements were made using the systematic scanning method. The analysis included the determination of basic stereometric parameters from the amplitude group and roughness together with isometric visualization.

RESULTS AND DISCUSSION OF TESTS

Influence of electrolyte temperature and current density on anodising voltage

Figure 2 shows voltage changes over time during anodising. The characteristics presented in Figure 2a

show that the formation of layers in an electrolyte at a lower temperature causes higher voltages during anodising. It can also be concluded that the trend of voltage characteristics for each temperature is similar.

Figure 2b shows the diagram of the dependence of the anodising voltage on time for three current densities at a constant electrolyte temperature of 292 K. Voltages increase as current density increases. The highest initial voltages were found for the highest current density of 4 A/dm², and the lowest were found for a current density of 2 A/dm². The differences in the initial voltage values are not significant, and they amount to 2–5 V and increase with the anodising time.

Surface geometric structure (SGS) analysis

Tables 3 and 4 list the amplitude parameters of the surface geometric structure before the tribological tests (Table 3) and after the tribological tests (Table 4). The values of amplitude parameters of all specimens significantly decreased after the tribological test as a result of the application of a sliding film on the surface.

Figures 3–7 show the surface geometric structure before the tribological test (3a, 4a, 5a, 6a, 7a) and after the tribological test with an applied film (3b, 4b, 5b, 6b, 7b) for various parameters of oxide layer formation. The isometric images presented below show that surface roughness after the tribological test decreases for all tested surfaces, causing their smoothing.

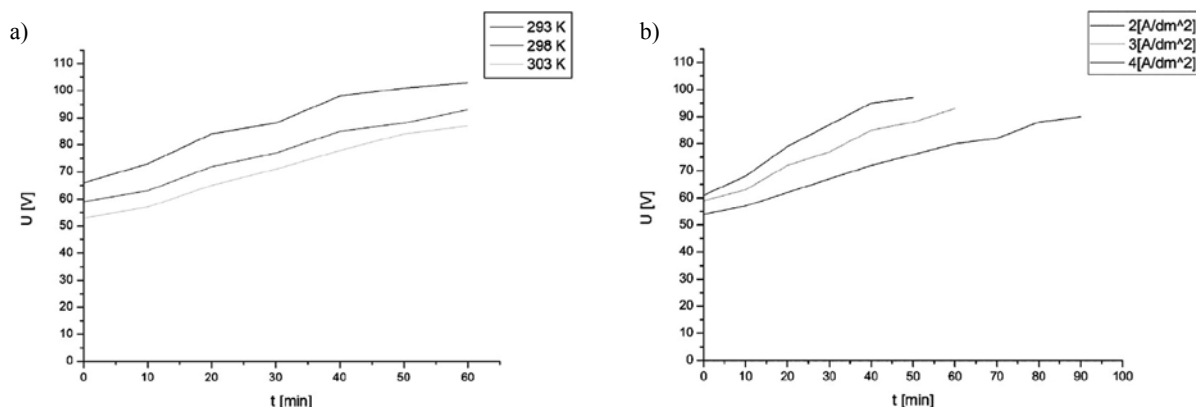


Fig. 2. Diagram of the dependence of anodising voltage on the duration of the process: a) for a current density of 3 [A/dm²] for various electrolyte temperatures, b) for an electrolyte temperature of 298 K for three current densities

Rys. 2. Wykres zależności napięcia anodowania od czasu procesu: a) dla gęstości prądowej 3 [A/dm²] dla różnych temperatur elektrolitu, b) dla temperatury elektrolitu 298 K dla trzech gęstości prądowych

Table 3. Amplitude parameters of surface geometric structure before the tribological test

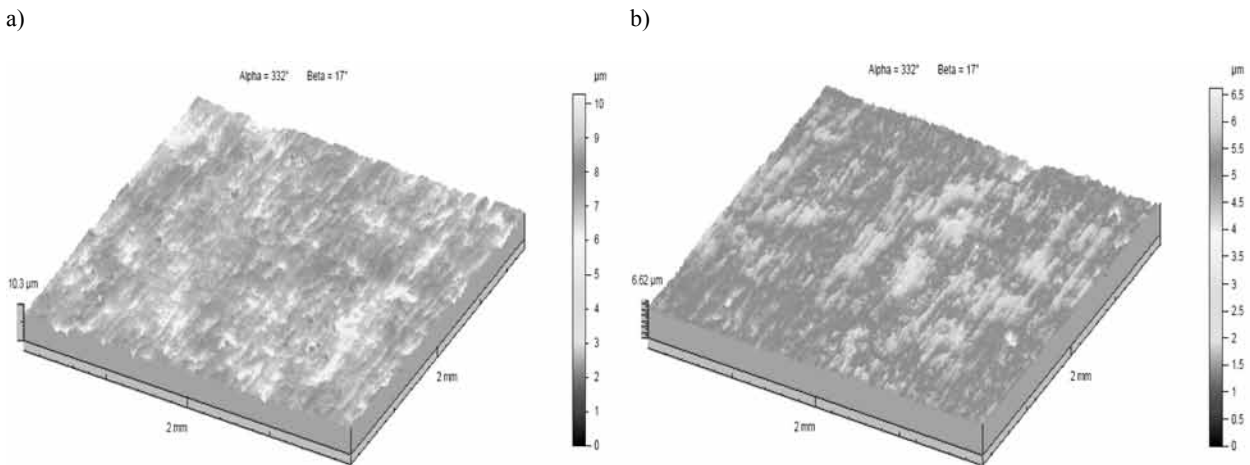
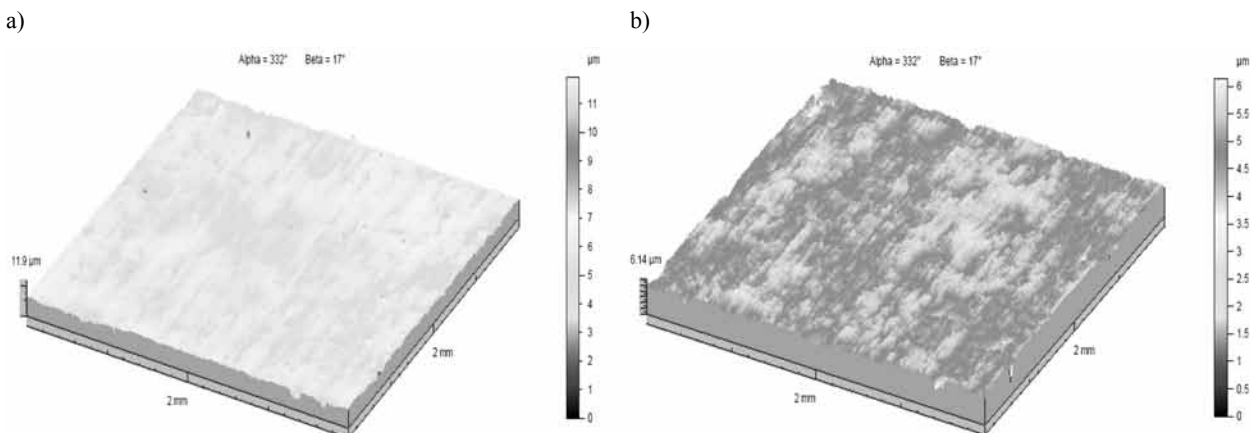
Tabela 3. Parametry amplitudowe struktury geometrycznej powierzchni przed wykonaniem testu tribologicznego

Determination of the counter-specimen	Sa [μm]	Sq [μm]	Sp [μm]	Sv [μm]	St [μm]
A	0.425	0.601	3.39	6.9	10.3
B	0.424	0.583	6.26	5.68	11.9
C	0.649	0.907	10.9	7.78	18.7
D	0.582	0.782	3.66	7.44	11.1
E	0.456	0.647	5.39	10.6	16

Table 4. Amplitude parameters of surface geometric structure after the tribological test

Tabela 4. Parametry amplitudowe struktury geometrycznej powierzchni po wykonaniu testu tribologicznego

Determination of the counter-specimen	Sa [μm]	Sq [μm]	Sp [μm]	Sv [μm]	St [μm]
A	0.326	0.454	1.34	5.28	6.62
B	0.303	0.407	1.12	5.02	6.14
C	0.364	0.486	2.45	5.12	7.57
D	0.337	0.473	1.52	5.23	6.75
E	0.34	0.454	1.36	6.62	7.98

**Fig. 3. Isometric images of the surface of oxide layers formed in an electrolyte at a temperature of 293 K and current density of 3 A/dm²: a) before the tribological test, b) after the tribological test**Rys. 3. Izometryczne obrazy powierzchni warstw tlenkowych wytwarzanych w elektrolicie o temperaturze 293 K przy gęstości prądowej 3 A/dm²: a) przed testem tribologicznym, b) po teście tribologicznym**Fig. 4. Isometric images of the surface of oxide layers formed in an electrolyte at a temperature of 298 K and current density of 3 A/dm²: a) before the tribological test, b) after the tribological test**Rys. 4. Izometryczne obrazy powierzchni warstw tlenkowych wytwarzanych w elektrolicie o temperaturze 298 K przy gęstości prądowej 3 A/dm²: a) przed testem tribologicznym, b) po teście tribologicznym

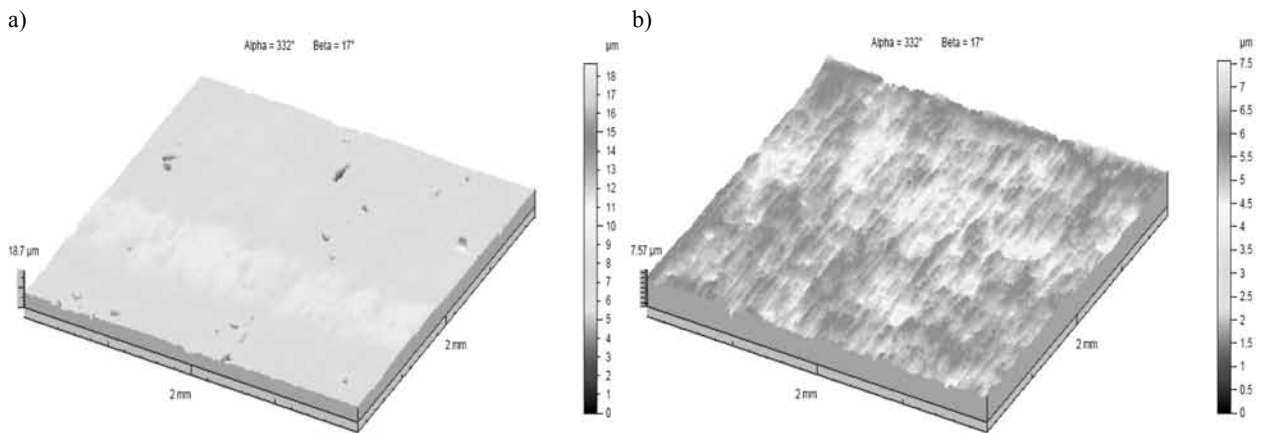


Fig. 5. Isometric images of the surface of oxide layers formed in an electrolyte at a temperature of 303 K and current density of 3 A/dm²: a) before the tribological test, b) after the tribological test

Rys. 5. Izometryczne obrazy powierzchni warstw tlenkowych wytwarzanych w elektrolicie o temperaturze 303 K przy gęstości prądowej 3 A/dm²: a) przed testem tribologicznym, b) po teście tribologicznym

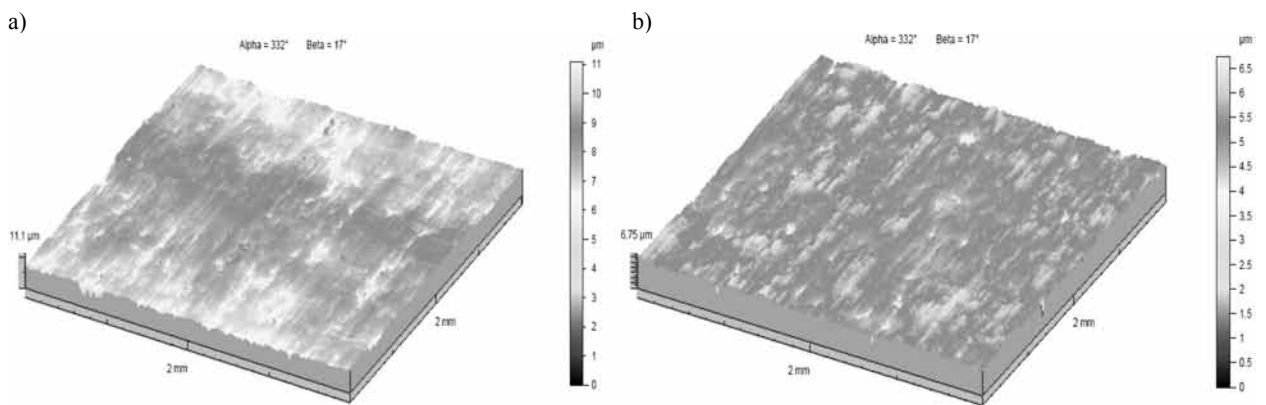


Fig. 6. Isometric images of the surface of oxide layers formed in an electrolyte at a temperature of 298 K and current density of 2 A/dm²: a) before the tribological test, b) after the tribological test

Rys. 6. Izometryczne obrazy powierzchni warstw tlenkowych wytwarzanych w elektrolicie o temperaturze 298 K przy gęstości prądowej 2 A/dm²: a) przed testem tribologicznym, b) po teście tribologicznym

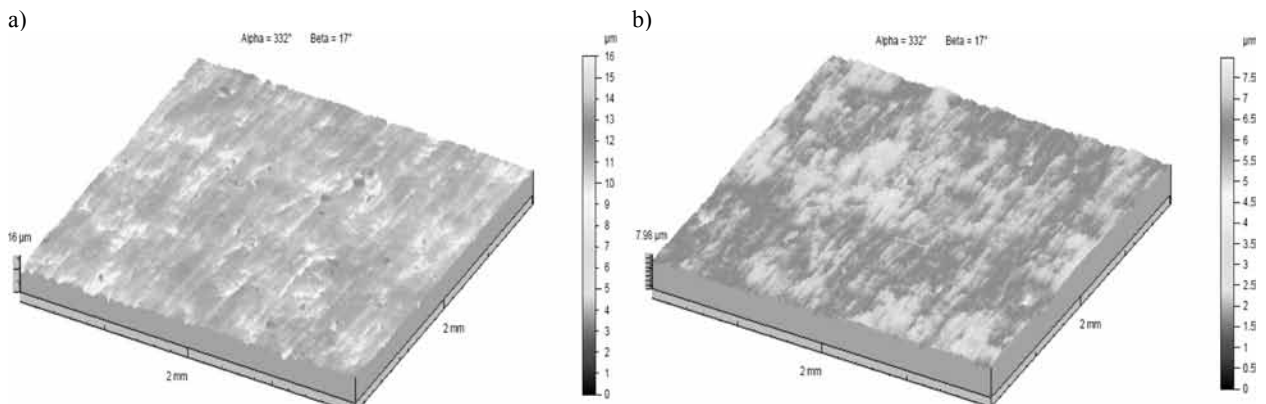


Fig. 7. Isometric images of the surface of oxide layers formed in an electrolyte at a temperature of 298 K and current density of 4 A/dm²: a) before the tribological test, b) after the tribological test

Rys. 7. Izometryczne obrazy powierzchni warstw tlenkowych wytwarzanych w elektrolicie o temperaturze 298 K przy gęstości prądowej 4 A/dm²: a) przed testem tribologicznym, b) po teście tribologicznym

Surface free energy analysis

SFE results were calculated using the van Oss-Chaunhury-Good method. The influence of the temperature of the electrolyte on the surface free energy is shown in Figure 8a, and Figure 8b shows the influence of current density on SFE. The surface free energy increases proportionally to parameter S_p , which specifies the maximum height of surface elevation, and to parameter S_r , which corresponds to the height of surface irregularities. This means that a layer with significant surface elevations and with surface irregularities has a higher SFE value. The value of the surface free energy also changes depending on the current density of oxide layer formation. Its value increases inversely in proportion to the current density during anodising. A correlation between the electrolyte temperature and SFE value was also observed. As the temperature of the electrolyte increases, the surface free energy also increases.

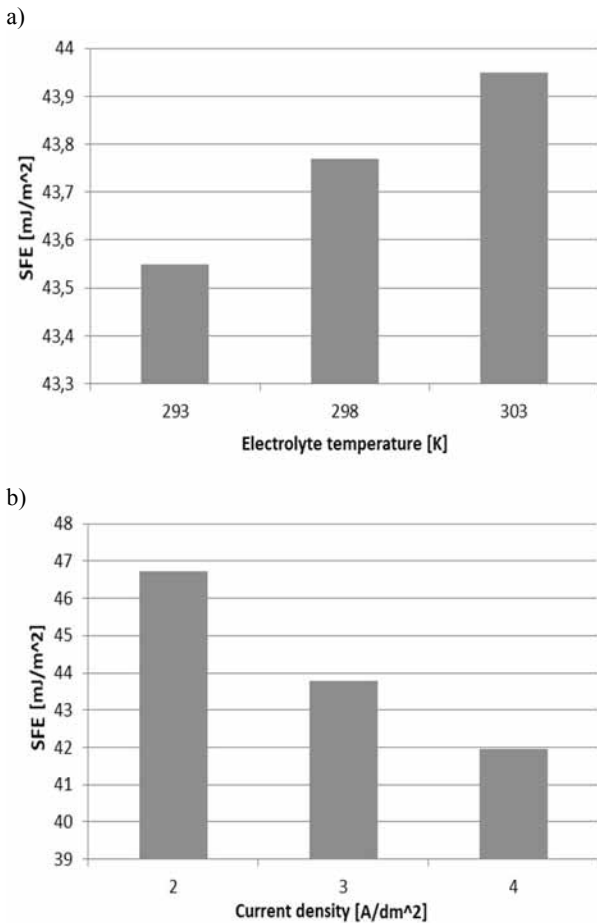


Fig. 8. Influence of anodising parameters on surface free energy: a) electrolyte temperature for a current density of 3 A/dm², b) current density for an electrolyte temperature of 298 K

Rys. 8. Wpływ parametrów anodowania na swobodną energię powierzchniową: a) temperatury elektrolitu dla gęstości prądu 3 A/dm², b) gęstości prądu dla temperatury elektrolitu 298 K

Analysis of layer surface morphology

Figure 9 shows the morphology of the surface of Al₂O₃ layers formed on an aluminium alloy with a current density of 3 A/dm² at different electrolyte temperatures (293 K, 298 K, and 303 K). The attached images show that the size and shape of pores change with the temperature of the electrolyte.

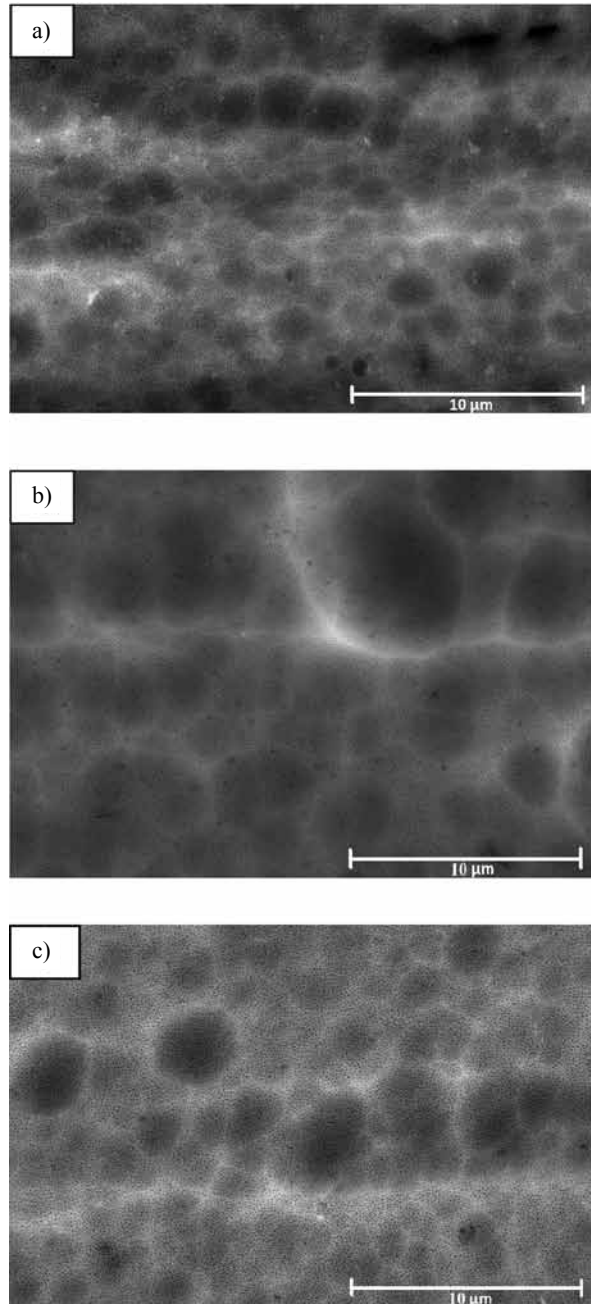


Fig. 9. Image of the surface morphology of oxide layers formed in an electrolyte at a current density of 3 A/dm² and electrolyte temperature of: a) 293 K, b) 298 K, c) 303 K

Rys. 9. Obraz morfologii powierzchni warstw tlenkowych wytwarzanych w elektrolicie o gęstości prądowej 3 A/dm² przy temperaturze elektrolitu: a) 293 K, b) 298 K, c) 303 K

Figure 10 shows the microstructure of T7W used in tribological tests. **Figure 10a** shows the surface of the specimen before the tribological test, and **Figure 10b** shows the surface of the specimen after the test. **Figure 10b** shows fragments with a smooth surface.

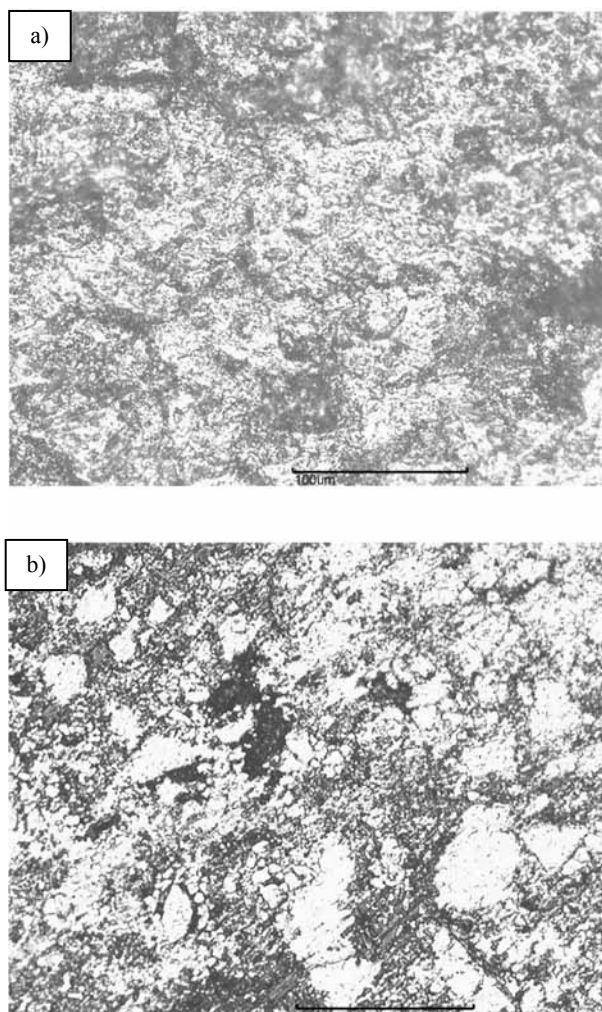


Fig. 10. Microstructure of T7W: a) before tribological test, b) after tribological test

Rys. 10. Mikrostruktura tworzywa T7W: a) przed testem tribologicznym, b) po teście tribologicznym

Analysis of microhardness

In order to determine the hardness of the oxide layer, which depend on the manufacturing parameters, microhardness was measured using the Vickers method, which consists in pressing a diamond pyramid with a square base into an aluminium oxide layer.

Figure 11 shows the influence of the electrolyte temperature and current density during oxide layer formation on its microhardness. The value of microhardness (**Fig. 11a**) increases inversely in proportion to the temperature of the electrolyte. The highest differences in hardness were found between the

layers formed in the electrolyte with a temperature of 298 K and 303 K. The highest value of microhardness (**Fig. 11b**) was found for a layer formed at a current density of 3 A/dm².

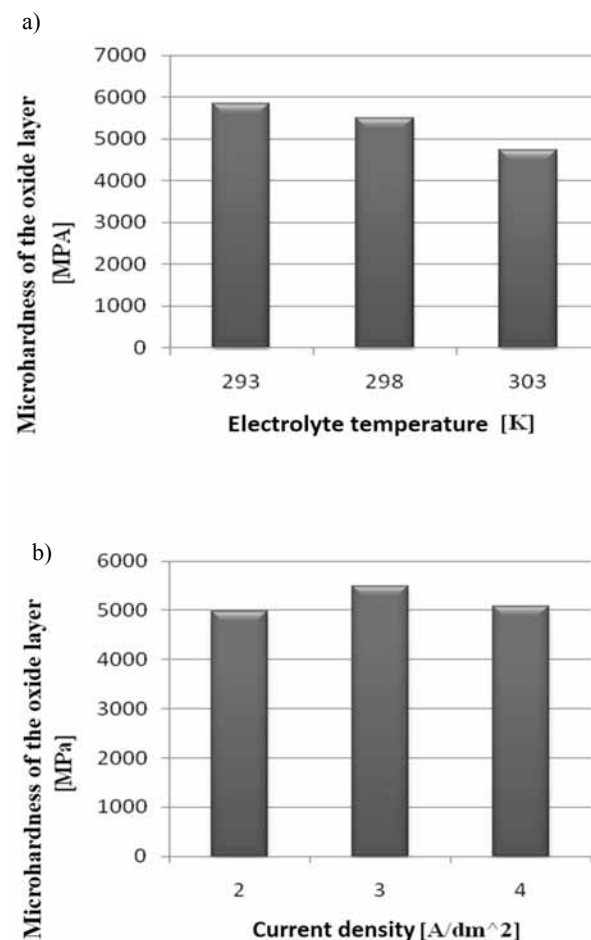


Fig. 11. Influence of anodising parameters on layer microhardness: a) electrolyte temperature for a current density of 3 A/dm², b) current density for an electrolyte temperature of 298 K

Rys. 11. Wpływ parametrów anodowania na mikrotwardość warstwy: a) temperatury elektrolitu dla gęstości prądu 3 A/dm², b) gęstości prądu dla temperatury elektrolitu 298 K

Analysis of tribological properties

Figure 12 shows the influence of oxide layer formation parameters in a couple with T7W on the value of friction coefficient μ . **Figure 12a** illustrates the correlation between the electrolyte temperature and the value of the friction coefficient. Friction coefficient μ is inversely proportional to the electrolyte temperature increase and is therefore also inversely proportional to the SFE value.

Figure 13 shows the influence of the parameters of oxide layer formation on linear wear Z_1 of the friction node. The value of the linear wear of the friction node changes proportionally to the electrolyte temperature

(Fig. 13a) and current density (Fig. 13b). An increase in electrolyte temperature and current density during anodising causes an increase in the linear wear of the oxide layer. A correlation between the change in the amount of SFE and the linear wear of the friction node

can also be observed. The amount of the surface free energy is directly proportional to linear wear Z_1 when the electrolyte temperature is increased and inversely proportional to linear wear Z_1 when current density is increased.

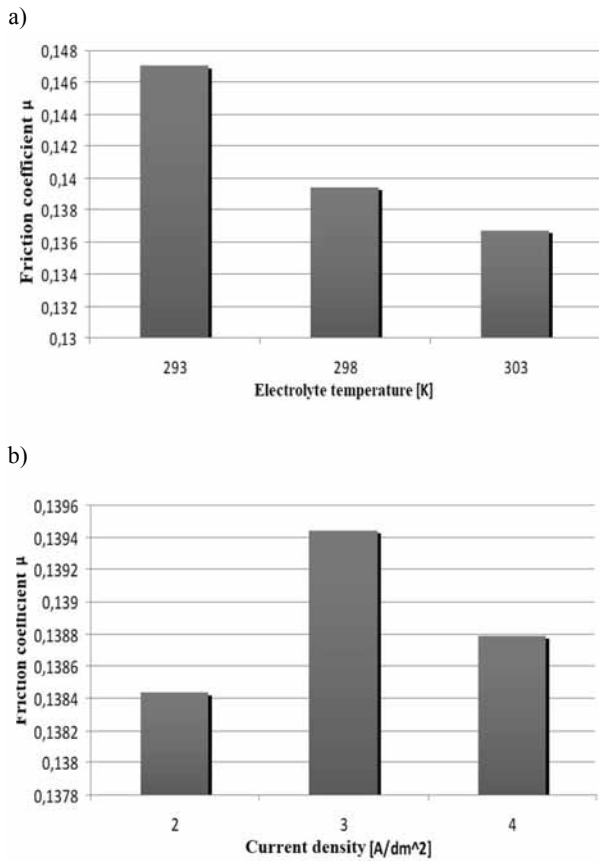


Fig. 12. Influence of anodising parameters on the value of friction coefficient μ of a sliding couple: a) electrolyte temperature for a current density of 3 A/dm², b) current density for an electrolyte temperature of 298 K

Rys. 12. Wpływ parametrów anodowania na wartość współczynnika tarcia μ skojarzenia ślizgowego: a) temperatury elektrolitu dla gęstości prądu 3 A/dm², b) gęstości prądu dla temperatury elektrolitu 298 K

CONCLUSIONS

The studies showed the dependence of the amount of surface free energy on the conditions of oxide layer formation and the influence on tribological properties of the layers. The greatest dependence of surface free energy can be observed in relation to linear wear Z_1 and the value of friction coefficient μ . Linear wear Z_1 increases as SFE decreases, so the greater the surface free energy, the lower the linear wear. On the other hand, the value of friction coefficient μ changes inversely in proportion to SFE. It was also observed that the anodising voltage increases proportionally to the increase in current density and inversely in proportion to the electrolyte temperature.

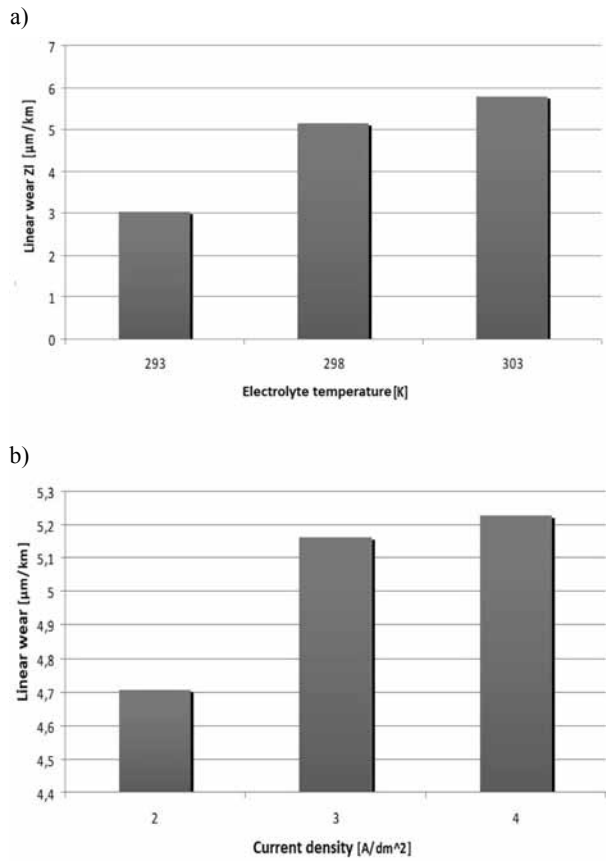


Fig. 13. Influence of electrolyte temperature and current density on linear wear Z_1 for: a) current density of 3 A/dm² at different electrolyte temperatures, b) temperature of 298 K at three current densities

Rys. 13. Wpływ temperatury elektrolitu i gęstości prądowej na zużycie liniowe Z_1 dla: a) gęstości prądowej 3 A/dm² przy różnych temperaturach elektrolitu, b) temperatury 298 K przy trzech gęstościach prądowych

The surface geometric structure changes depending on anodising conditions. It can be conclusively stated that the tribological test affects the amplitude parameters of SGS and surface roughness. The values of parameters S_p and S_t increase along with the increase in the electrolyte temperature during anodising. These parameters proportionally influence the value of surface free energy. The porosity of the layers increases along with the increase in the electrolyte temperature, which causes changes in the surface geometric structure. It would be advisable to carry out the anodising process for wider parameters (for a current density of 1 A/dm² and electrolyte temperature of 283 K) in order to better show the correlation between individual tribological parameters and surface free energy.

REFERENCES

1. Mokhtari S., Karimzadeh F., Abbasi M.H., Raeissi K.: Development of super-hydrophobic surface on Al 6061 by anodizing and the evaluation of its corrosion behavior, *Surf. Coat. Tech.* 324 (2017) 99–105.
2. Bara M.: Ocena wpływu przygotowania podłoża na właściwości tribologiczne nanoceramicznych warstw tlenkowych, *Tribologia* 4 (2014) 9–20.
3. Bara M., Kmita T., Korzekwa J.: Microstructure and properties of composite coatings obtained on aluminium alloys, *Arch. Metall. Mater.* 61(3) (2016) 1107–1112.
4. Szulc S., Stefko A.: *Obróbka powierzchniowa części maszyn - podstawy fizyczne i wpływ na własności użytkowe.* Warszawa: WNT, 1976.
5. Ghanbari A., Attar M.M.: Surface free energy characterization and adhesion performance of mild steel treated based on zirconium conversion coating: A comparative study, *Surf. Coat. Tech.* 246 (2014) 26–33.
6. Sobolewski S., Lodes M.A., Rosiwal S.M., Singer R.F.: Surface energy of growth and seeding side of free standing nanocrystalline diamond foils, *Surf. Coat. Tech.* 232 (2013) 640–644.
7. Schuster J.M., Schvezova C.E., Rosenberger M.R.: Effect of the contact angle on the morphology, residence time distribution and mass transfer into liquid rivulets: A CFD study, *Chemical Engineering Science*, 176 (2018) 356–366.
8. Thieme M., Worch H.: Ultrahydrophobic aluminium surfaces: properties and EIS measurements of different oxidic and thin-film coated states, *J. Solid State Electrochem.* 10 (2006) 737–745.
9. Wojciechowski L., Nosal S.: The application of free surface energy measurement to valuation of adhesive scuffing, *Maintenance and Reliability* 1 (2010) 83–89.